applied sciences

MDPI

Article

Sulfuric Acid Resistance of CNT-Cementitious Composites

Gun-Cheol Lee [1,†], Youngmin Kim [1,†], Soo-Yeon Seo [1], Hyun-Do Yun [2] and Seongwon Hong [3,*]

[1] Department of Architectural Engineering, Korea National University of Transportation, Chungju, Chungbuk 27469, Korea; gclee@ut.ac.kr (G.-C.L.); imkym97@ut.ac.kr (Y.K.); syseo@ut.ac.kr (S.-Y.S.)
[2] Department of Architectural Engineering, Chungnam National University, Daejeon, Chungnam 34134, Korea; wiseroad@cnu.ac.kr
[3] Department of Safety Engineering, Korea National University of Transportation, Chungju, Chungbuk 27469, Korea
* Correspondence: shong@ut.ac.kr; Tel.: +82-43-841-5339
† Both authors contributed equally to this manuscript and are dual first authors.

Abstract: This study analyzed changes in the durability characteristics of cement mortar incorporating carbon nanotube (CNT) and the electrical properties subjected to deterioration induced by sulfate attack. Powder types of multi-walled or single-walled CNTs were used and added to the composites with 1.0% and 2.0% mass fraction, and the specimens were immersed in 5% and 10% sulfuric acid solutions to investigate the durability of CNT cementitious composites. Although mechanical performance decreased due to relatively large pores (370–80 μm) caused by CNTs, specimens incorporating CNTs exhibited enhanced resistance to sulfuric acid as CNTs, which offered strong resistance to acid corrosion, and prevented contact between the cement hydrate and the sulfuric acid solution. Therefore, it is expected that self-sensing performance was exhibited because there were no significant differences in the electrical properties of cement mortar subjected to the deterioration by sulfate attack.

Keywords: cementitious composites; carbon nanotube (CNT); multi-walled CNT; single walled CNT; self-sensing; durability; sulfate attack

Citation: Lee, G.-C.; Kim, Y.; Seo, S.-Y.; Yun, H.-D.; Hong, S. Sulfuric Acid Resistance of CNT-Cementitious Composites. *Appl. Sci.* **2021**, *11*, 2226. https://doi.org/10.3390/app11052226

Academic Editor: Chul-Woo Chung

Received: 2 February 2021
Accepted: 27 February 2021
Published: 3 March 2021

1. Introduction

Concrete structures have inevitably suffered from the damage and degradation resulting from aging over a period of years, or external mechanical and environmental impacts during the service period. Therefore, to safely use them, structural health assessments and diagnosis are required by using evaluation equipment and devices. However, as structures have become larger, higher and more complex, this has been difficult because it is impossible to access the damaged area and degradation location in the concrete structures for safety reasons. To address these problems, structural health monitoring (SHM) systems have been developed and widely employed around the world [1–4]. In addition to SHM systems, self-monitoring or self-sensing composites have been developed and used to evaluate the damage of structures [5–20]. Steel fibers have been employed not only to increase the tensile strength of structures but also to provide self-sensing properties (Choi et al., 2019 [21]; Lee et al., 2018 [22]; Lee et al., 2017 [23]). Recently, there has been a growing interest in using carbon nanotubes (CNTs) as self-sensing materials of concrete due to their excellent electrical conductivity (Yoon et al., 2020 [24]; Choi et al., 2020 [25]). These studies mainly focused on structures on the ground, such that there is little research on self-sensing structures located in the ocean and underground. Furthermore, since sewage structures susceptible to chemical erosion constitute about 30% of the national urban infrastructures and are highly likely to suffer corrosion due to sulfuric acid attack, it was essential to provide them with self-sensing capabilities to detect damage. Generally, sulfate ions can easily penetrate into micro-voids and micro-cracks in concrete composites by the transfer mechanism and react with calcium aluminate hydrate and calcium hydroxide to produce expansion hydration

products including ettringite and gypsum, which results in the swelling of mixtures, bigger size cracks, and the loss of the mechanical properties of concrete [26–32]. This mechanism is called external sulfate attack [33–35]. When concrete is exposed to sulfate ions, thaumasite is formed as an alteration of cementitious composites and has very low strength, resulting in the disintegration of the cement paste [36].

CNTs have a significantly low density (1.3–1.4 g/cm^3) and the amount of CNTs does not exceed up to 2.0% of the weight of the binder (Yun et al., 2020 [37]; Lee et al., 2020 [38]). Moreover, it is very difficult to obtain uniform dispersion of CNTs in the matrix due to van der Waals forces between the CNT particles, and the poor dispersion of CNTs results in low mechanical properties of the cementitious composites. There exist diverse techniques and methods, such as admixtures, silica fume, surface modification of CNT, minimizing the water-to-binder ratio, and ultrasonication to improve homogeneous dispersion in the composites and their mechanical strength [39–51]. Moreover, uniformly dispersed CNT cementitious composites have excellent self-sensing performance. In spite of numerous studies on the uniform dispersion of CNT cementitious composites, to the authors' knowledge, no one has conducted studies on the durability of CNT cementitious composites subjected to sulfate attack.

In this research, to investigate the durability of CNT cementitious mixtures exposed to sulfate attack, powder types of multi-walled or single-walled CNTs were selected and added to the cement mortar with up to 2.0% mass fraction and the specimens were immersed in 5% and 10% sulfuric acid solutions. Several mechanical tests, including weight change ratio and compressive strength change ratio, were carried out before and after degradation induced by sulfate attack. Electrical resistance was measured to evaluate the electrical performance of the composites, and mercury intrusion porosimetry (MIP) and scanning electron microscopy (SEM) tests were conducted to examine the porosity of the cementitious composites before and after the sulfate damage.

2. Experimental Programs

2.1. Materials and Mixture Proportions

Ordinary Portland cement (OPC, Type I KS L 5201 [52]), powder-type single-walled (SW) and multi-walled (MW) CNTs, and standard sand (KS L ISO 679 [53]) were employed to fabricate CNT cementitious composites. Tables 1 and 2 show the chemical and physical properties of OPC and physical properties of CNTs, respectively. Figure 1 shows powder-type SWCNT and MWCNT, and their schematics. The particle size distribution of standard sand is summarized in Table 3. The mixture proportions of CNT mortar are provided in Table 4 in detail. The amount of CNT in cementitious composites was determined based on previous studies (Yun et al., 2020 [37]; Lee et al., 2020 [38]). The poly carboxylate-based high-performance water reducing agent (KS F 2560 [54], Chemical Admixtures) was added in cementitious composites, as summarized in Table 1. To improve workability and uniform dispersion of SWCNT in the composites, the mixing time was increased by an additional 30 s. The specimens were fabricated, and tests were conducted in accordance with KS L ISO 679 [53].

Table 1. Chemical and physical properties of ordinary Portland cement (OPC).

Chemical Properties (%)					Physical Properties	
SiO_2	Al_2O_3	Fe_2O_3	CaO	MgO	Density(g/cm^3)	Fineness(cm^2/g)
22.23	5.21	3.38	64.58	2.3	3.15	3300

Table 2. Physical properties of carbon nanotubes (CNTs).

Item	MWCNT	SWCNT
Diameter (ηm)	5~100	1.2~3.0
Length (μm)	10	10
Tension (GPa)	<50	~45
Electrical resistance ($\Omega \cdot m^2$)	5.1×10^{-6}	10×10^{-4}
Thermal conductivity (W/m·K)	Max. 3000	Max. 6000
Specific surface area (m^2/g)	130~160	700~900

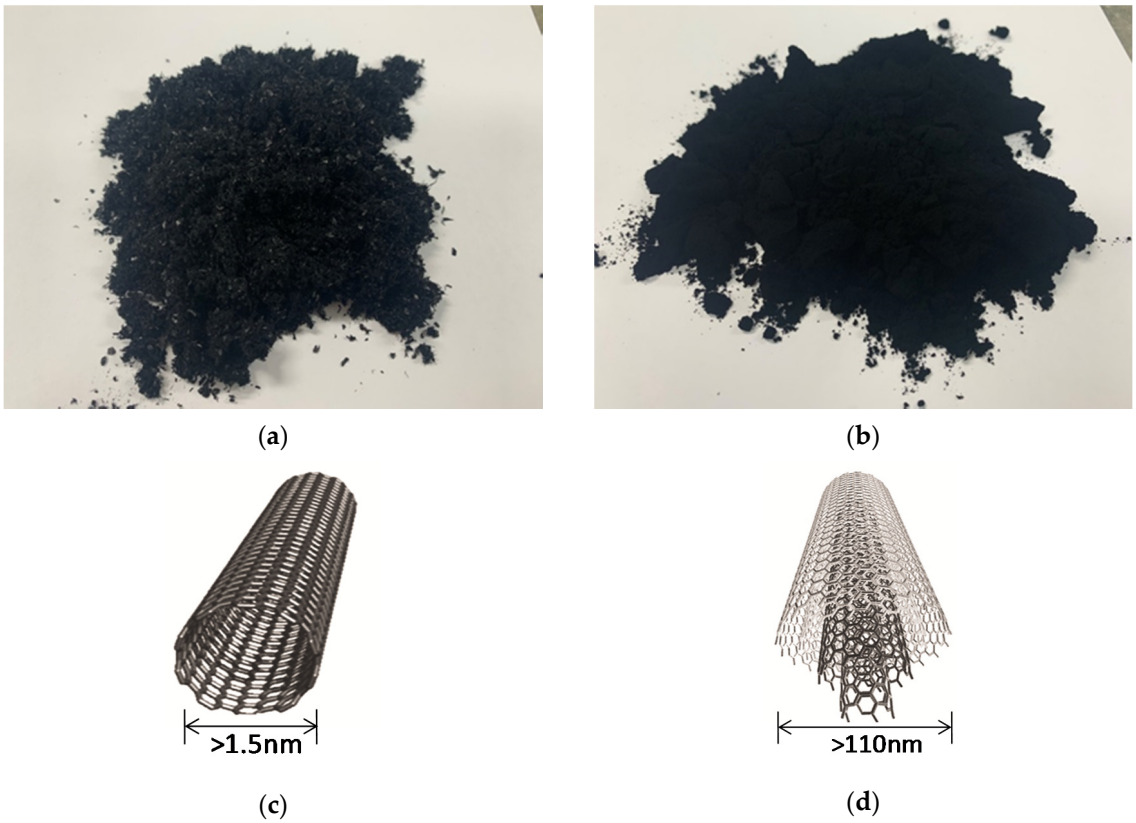

Figure 1. Picture of powder-type carbon nanotubes: (**a**) single-walled carbon nanotubes (SWCNTs); (**b**) multi-walled carbon nanotubes (MWCNTs); (**c**) schematics of SWCNTs; (**d**) Schematics of MWCNTs.

Table 3. Particle size distribution of standard sand (KS L ISO 679 [53]).

Size (mm)	2.0	1.6	1.0	0.5	0.16	0.08
Percent finer (%)	0	8	35	70	90	99

Table 4. Mixture proportion of cement mortar.

Sample	W/C	Weight (kg/m^3)				Admixture (%)	
		Cement	Water	Sand *	CNT	MWCNT	SWCNT
CNT 0	0.5	510	255	1530	0	0	0
CNT 0.5				1530	2.55	0	2
CNT 1.0				1530	5.10	2	6
CNT 2.0				1530	10.2	4	14

* Standard sand (KS L ISO 679 [53]).

2.2. Experimental Methods

The compressive and flexural strengths were measured. To identify resistance to sulfuric acid, the specimens were immersed in 5% or 10% sulfuric acid solution (Bellmann et al., 2006 [55]; Bae et al., 2010 [56]; Elyamany et al., 2018 [57]), and the weight change ratio, compressive strength change ratio, and electrical resistance change rate were observed. In addition, the porosity before and after the damage for 28 days caused by the sulfuric acid solution and its characteristics were analyzed based on MIP and SEM images.

To evaluate the chemical resistance of CNT cement mortar, three cylindrical specimens per test with a diameter of 100 mm and a height of 200 mm were made and stored for 24 h at a temperature of 20 ± 1 °C with humidity of 60 ± 1% and demolded in accordance with KS L ISO 679 [54]. Then, the specimens were cured in a water tank at 20 ± 1 °C for 28 days, dried for 24 h at a temperature of 80 ± 1 °C, and then immersed in 5% or 10% sulfuric acid solutions for 28 days according to JSTM C 7401 [58], as shown in Figure 2a. The position of the immersed specimens was rotated every 12 h, because when their surface was attached, it may influence deterioration. Changes in electrical resistance, weight change ratio, and compressive strengths were measured at 3, 7, and 28 days of immersion where the compressive strength change ratio (F_c) and weight change ratio (W_c) are determined by Equations (1) and (2).

$$F_c = \left(\frac{F_s - F_{ini}}{F_{ini}} \right) \times 100 \quad (1)$$

$$W_c = \left(\frac{W_s - W_{ini}}{W_{ini}} \right) \times 100 \quad (2)$$

where F_s is the compressive strength after damage by sulfuric acid (MPa), F_{ini} is the initial compressive strength after 28 days of water curing (MPa), W_s is the weight of the specimen after damage by sulfuric acid (g), and W_{ini} is the initial weight of the specimen after 28 days of water curing (g).

Figure 2. Immersion in sulfuric acid solution.

In accordance with KS L ISO 679 [53], a rectangular parallelepiped specimen with dimensions of 40 × 40 × 160 mm was fabricated, demolded after 24 h, and cured in water maintained at 20 ± 1 °C. The compressive and flexural strength tests of the CNT cement mortar were performed.

The same specimen with dimensions of 40 × 40 × 160 mm was used for measuring the electrical resistance of CNT cement mortar and its electrical resistance after damage by a sulfuric acid solution, and copper plates were inserted at both ends of the specimen (see Figure 3). Before the test, it was confirmed that the copper plates were not damaged by treatment with sulfuric acid for 28 days. The electrical resistance was measured in a 2-probe method using the data acquisition system DAQ970A with the program BenchVue) as presented in Figure 4. In addition, each measurement was made after drying for 24 h at a temperature of 80 ± 1 °C in a dryer because of the results of previous research (Kwon, 2009 [59]) showing that the moisture content affects the conductivity of cement mortar.

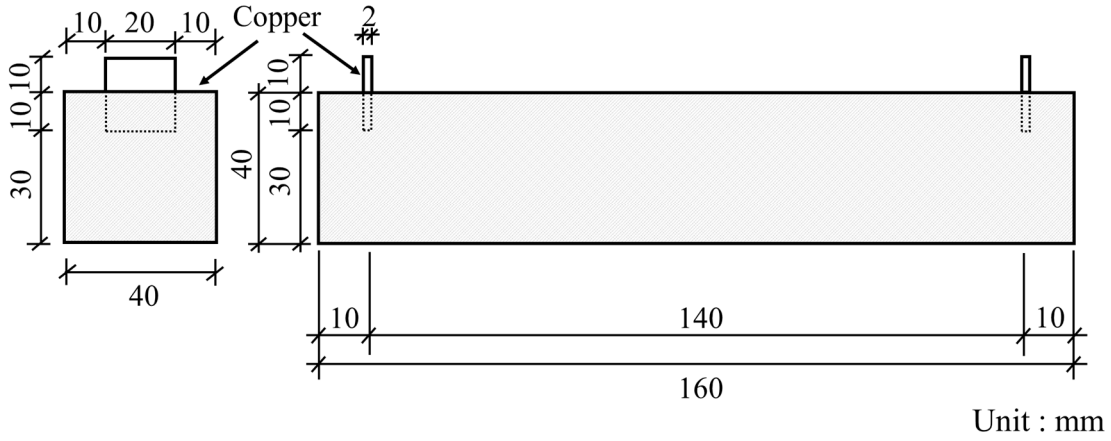

(**a**) Side and front view

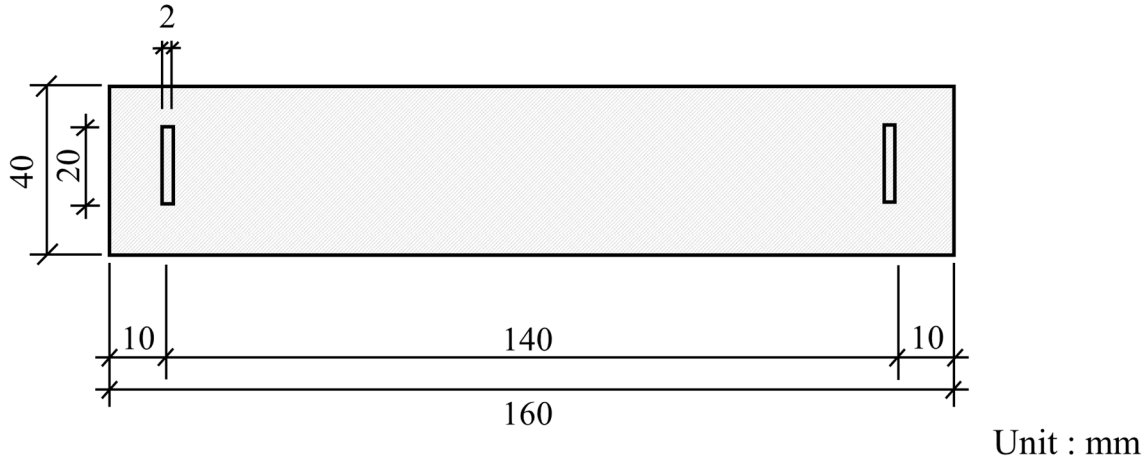

(**b**) Plan view

Figure 3. Dimension of rectangular parallelepiped specimen of cement mortar for electrical resistance test: (**a**) side view and front view; (**b**) plan view.

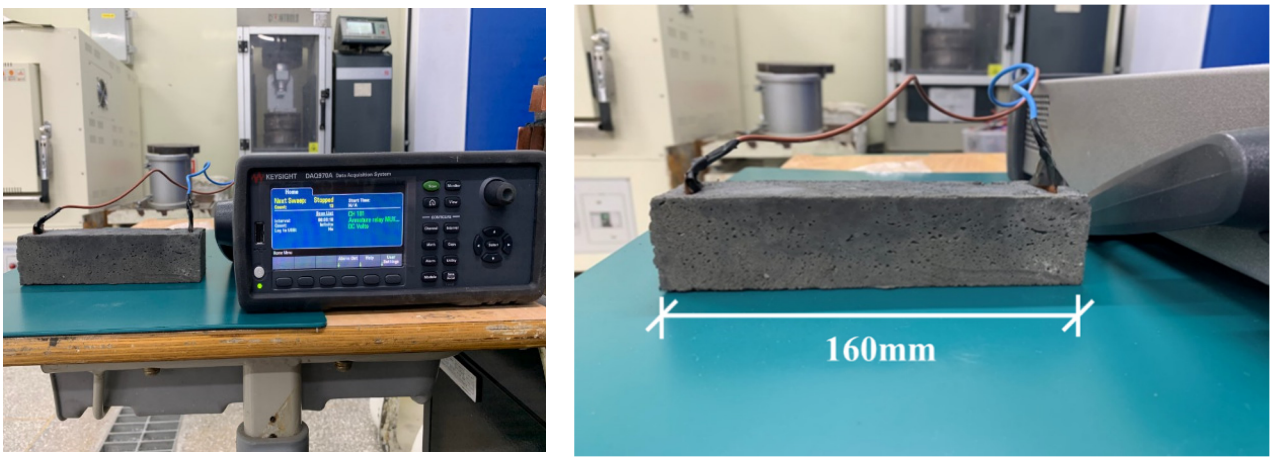

(**a**) (**b**)

Figure 4. Schematic of cementitious composites for electrical resistance test: (**a**) specimen and device; (**b**) side view.

To measure pore size distribution before and after the 28-day immersion of CNT cement mortar in a sulfuric acid solution, about 2 g of the sample immersed for 28 days was collected from the same location on the top end of the surface of the specimen (see Figure 5), because the most damaged area was the surface. The upper part of the samples damaged by sulfuric acid attack was first cut with a cutter to about 20 mm in size and then crushed with a small hammer for the SEM tests. In addition, MIP was utilized as an analytical technique using Autopore V 9600 (Figure 6) and was also used as damage identification due to crushing during the collection process of the composites.

Figure 5. Surface location of collected sample immersed for 28 days and collected samples.

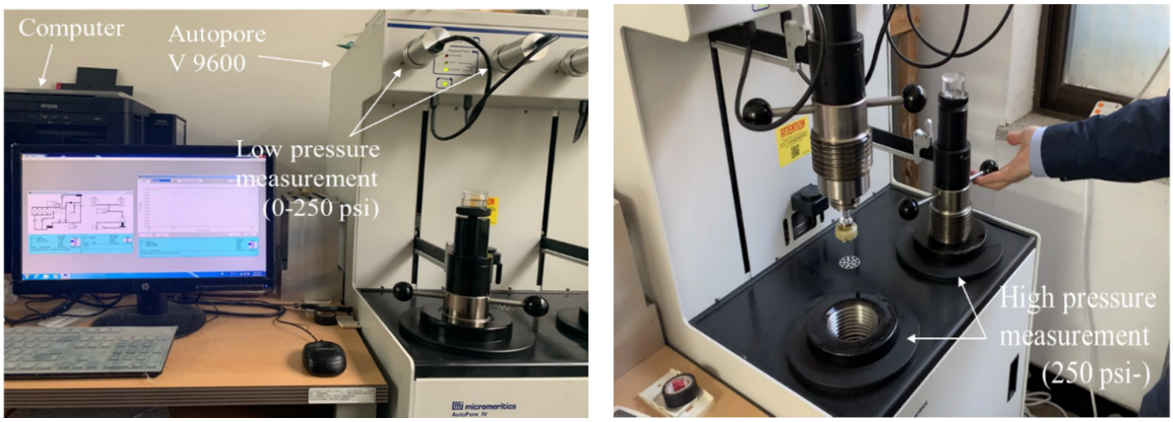

Figure 6. Experiment equipment for mercury porosimeter test.

3. Test Results and Discussion

3.1. Features of Sulfate Resistance

Figure 7 demonstrates the weight change ratio of CNT cementitious composites after immersion in a sulfuric acid solution. It was found that the weight change ratio decreased as the age increased. The weight of the plain specimen immersed in 5% sulfuric acid solution decreased rapidly after 7 days, while that of the plain specimen immersed in 10% sulfuric acid solution decreased in the early stage (by 7 days) of immersion. It is ascertained that deterioration occurred due to sulfuric acid erosion and the weight decreased because of the peeling and falling-off of the composites. However, as the amount of CNTs increased, a decrease in weight was more rarely found in the CNT cementitious composites than the plain composite.

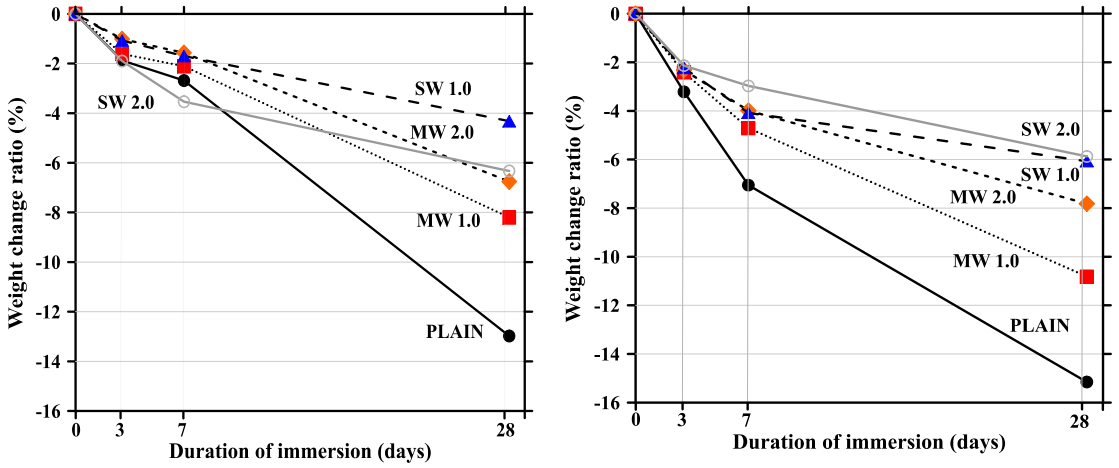

(**a**) 5% sulfuric acid solution (**b**) 10% sulfuric acid solution

Figure 7. Weight change ratio of cementitious composites immersed in sulfuric acid solution: (**a**) 5% and (**b**) 10%.

Figure 8 demonstrates the compressive strength change ratio after immersion in a sulfuric acid solution. The compressive strength change ratio showed a similar tendency to that of the weight decrease ratio. This is because deterioration occurred due to the reaction of sulfate ions with the cement hydrate, resulting in relaxation and breakage of the hydration structures.

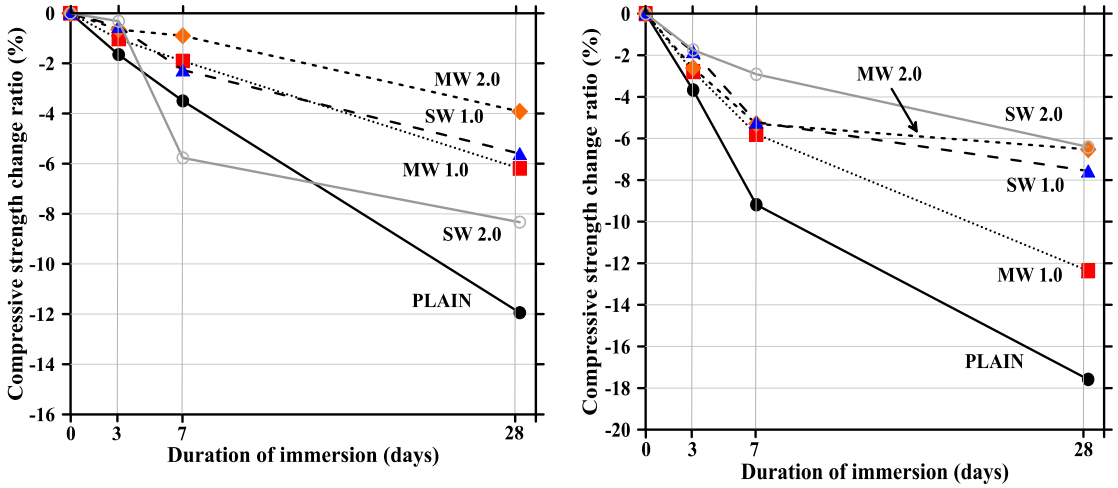

(**a**) 5% sulfuric acid solution (**b**) 10% sulfuric acid solution

Figure 8. Compressive strength change ratio of cementitious composites immersed in sulfuric acid solution: (**a**) 5% and (**b**) 10%.

The SEM photos of the specimen surface taken before and after the immersion of cement mortar in a sulfuric acid solution are exhibited in Figure 9. In particular, the SEM photos in Figure 9 were taken after immersion in a sulfuric acid solution for 28 days. The images were taken at 25 times magnification, which was enough to observe the degree of deterioration of the composite surface. The cement hydrate is a compound that is very vulnerable to acid, and huge damage occurred in the cement hydrate except for aggregate in the plain specimen after immersion in a sulfuric acid solution. However, in the case of the CNT cementitious composites, less damage occurred in the cement hydrate because the nanoparticles with excellent corrosion resistance to acid prevented contact between the cement hydrate and the sulfuric acid solution.

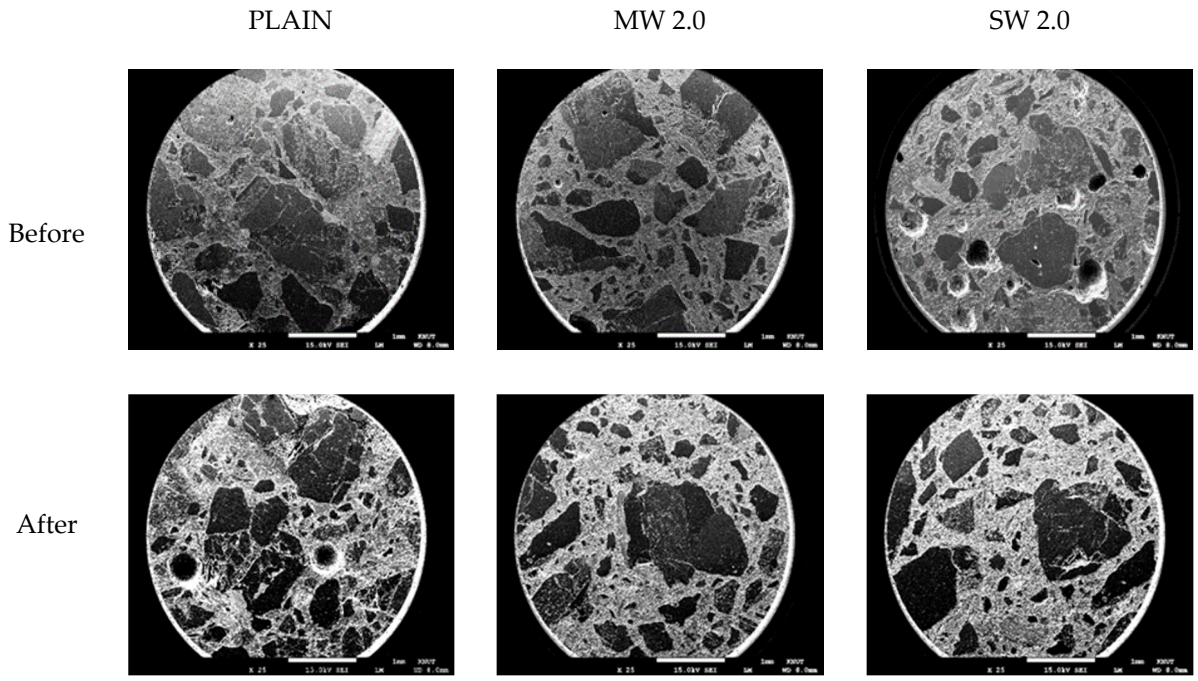

Figure 9. Scanning electron microscopy (SEM) images before and after damage by sulfuric acid attack.

3.2. Strength Properties

The compressive and flexural strengths of CNT cementitious composites are presented in Figure 10. It is shown that the CNT cementitious composites had a lower compressive and flexural strengths than the plain specimen. In particular, as the incorporation ratio increased, the compressive and flexural strengths of the SWCNT composites further decreased compared to those of the MW composites. This is because the hydrophobic CNTs were not properly dispersed in the cementitious composites, but exist as large pores. Moreover, the agglomeration and intorsion of the CNTs caused by the van der Waals forces in the composite was another factor that reduced the compressive and flexural strength (Lee et al., 2020 [38]). As the specimen with 2% SWCNT was not cured until the age of 7 days, it was impossible to measure its strength. This is because 10% chemical admixtures were only added to this specimen (SW 2.0) for workability, resulting in delayed curing.

3.3. Electric Resistance

Figure 11 shows the electrical resistance of cement mortar incorporating CNTs before and after deterioration caused by sulfuric acid. The electrical properties of the specimen before damage revealed that as the CNTs were incorporated, its resistance greatly decreased by up to 90%, and it was further decreased in SWCNT cementitious composites compared to MWCNT composites. This is because CNTs, which are conductive nanomaterials, were incorporated into the cementitious composites to give conductivity through which

electric current can flow, and the electrical resistance value was then reduced despite the bundle phenomenon due to the van der Waals force. It denotes that the CNT cementitious composites have self-sensing ability. In addition, it was found that the electrical resistance value increased after deterioration due to sulfuric acid attack. The electrical resistance of plain cement mortar significantly increased when immersed in a 10% sulfuric acid solution because an increase in pore area was induced by the hydrate relaxation, resulting in poor electrical conductivity. It was observed that there was a slight increase in the electrical resistance of the CNT cementitious mixtures because the disconnection between CNTs occurred in the composites as the deterioration progressed. However, it was ascertained that since there was no significant difference in conductivity, the self-sensing performance could be demonstrated.

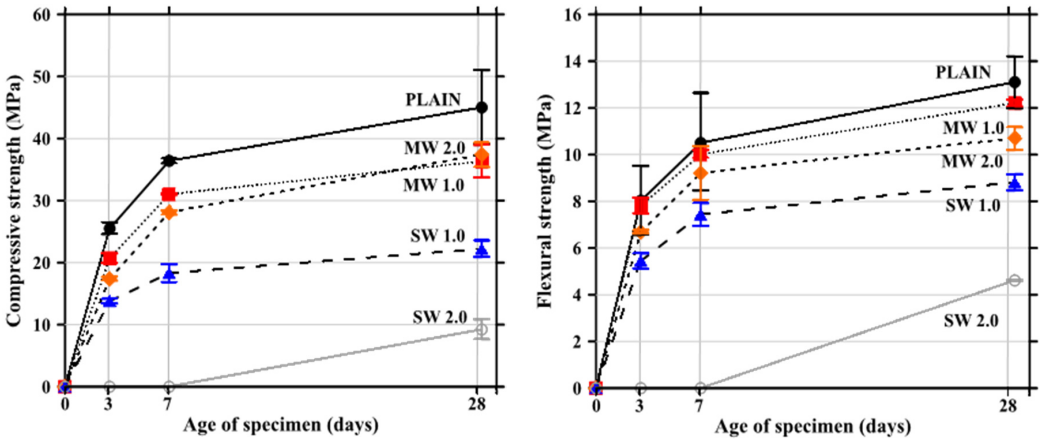

(**a**) Compressive strength (**b**) Flexural strength

Figure 10. Strength of carbon nanotube (CNT) cementitious composites: (**a**) compressive strength and (**b**) flexural strength.

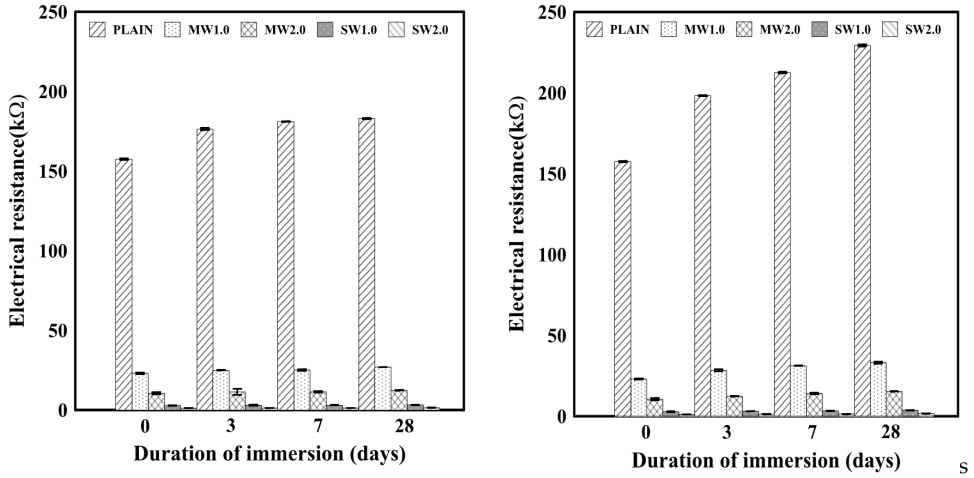

(**a**) 5% sulfuric acid solution (**b**) 10% sulfuric acid solution

Figure 11. Electrical resistance of CNT cementitious composites before and after deterioration by sulfuric acid: (**a**) 5% and (**b**)10%.

3.4. Pore Distribution Characteristics

The pore size distribution and cumulative pore volume of cement mortar incorporating CNTs before and after damage by 5% sulfuric acid solution are shown in Figures 12 and 13, respectively. As the incorporated amount of CNTs increased, relatively large pores with sizes ranging between 370 and 80 μm occurred (see Figure 11a). It was observed that the pore size was greater in the specimen incorporating SWCNT than MWCNT. These results

indicate that although the porosity was reduced due to the filling effect in the incorporation of CNTs with a nano-sized diameter of 1–100 nm, the hydrophobic CNTs were not uniformly dispersed in cementitious mixtures but exist in a bundled form. However, in the plain specimen, most of the pores with sizes ranging from 370 to 30 μm were distributed, and micro-pores (less than 1 μm) was not observed. These pores were originally filled with water remaining after mixing. As the water evaporated, these pores were created. Figure 12b depicts the pore distribution characteristics of the specimen after immersion in a sulfuric acid solution. The maximum pore diameter increased to 500 μm, and the distribution of larger pores than before was observed because the cement hydrate, which is vulnerable to chemical erosion, was dissolved in the sulfuric acid solution. This denotes that CNT cementitious composites had high resistance to chemical erosion, meaning that they helped to strengthen the cement hydrate structures. The pore distribution results in Figures 12 and 13 imply that as CNTs were incorporated, large pores were formed and could serve as easy paths for the sulfuric acid solution to penetrate. However, CNTs with excellent chemical resistance were attached to cement particles and prevented the penetration of ions such as cement hydrate, sulfate (SO_4^{2-}), and hydrogen (H^+), thereby improving the weight loss and strength reduction of the composites in Figure 6.

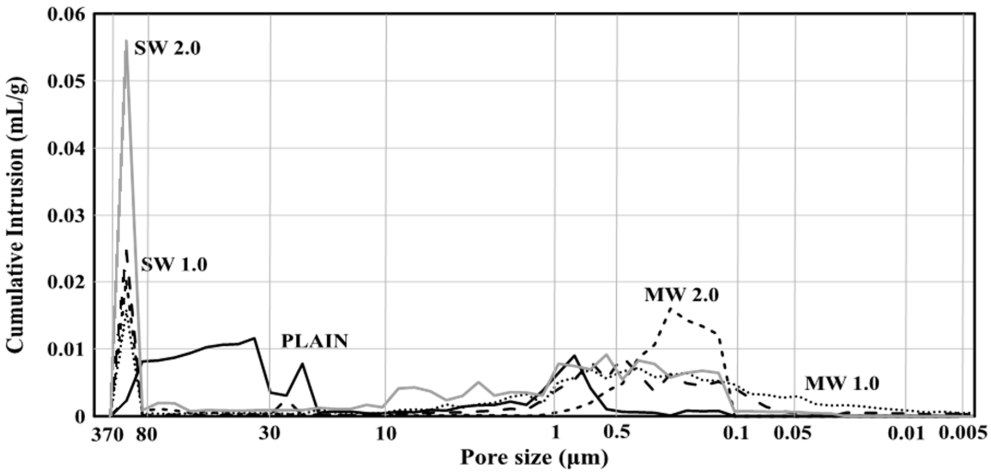

(**a**) Before damage

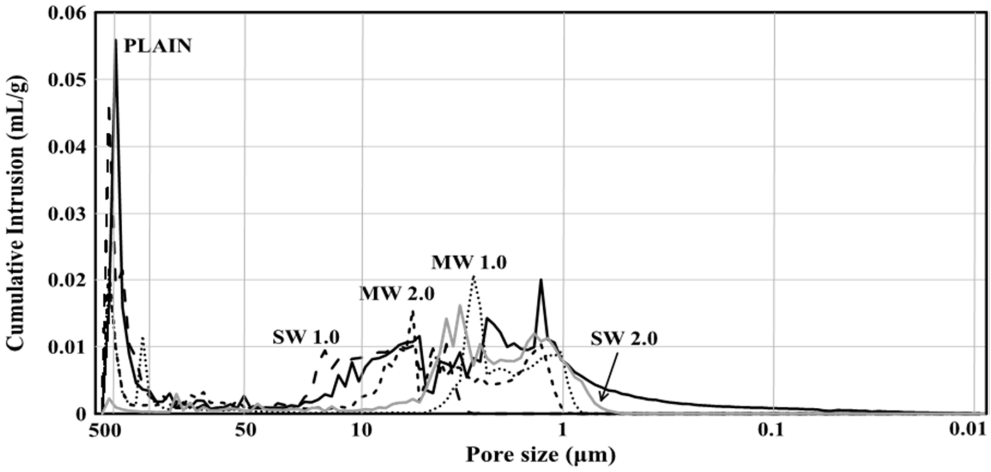

(**b**) After damage

Figure 12. Pore size distribution of CNT cementitious composites before and after immersion in 5% sulfuric solution: (**a**) before damage and (**b**) after damage.

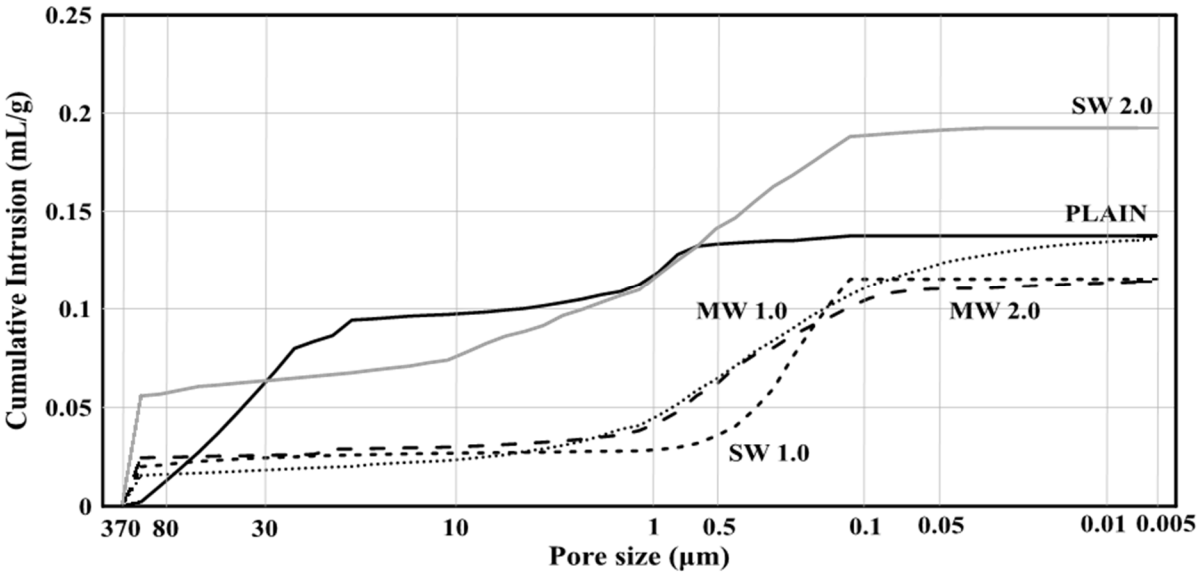

(**a**) Before damage

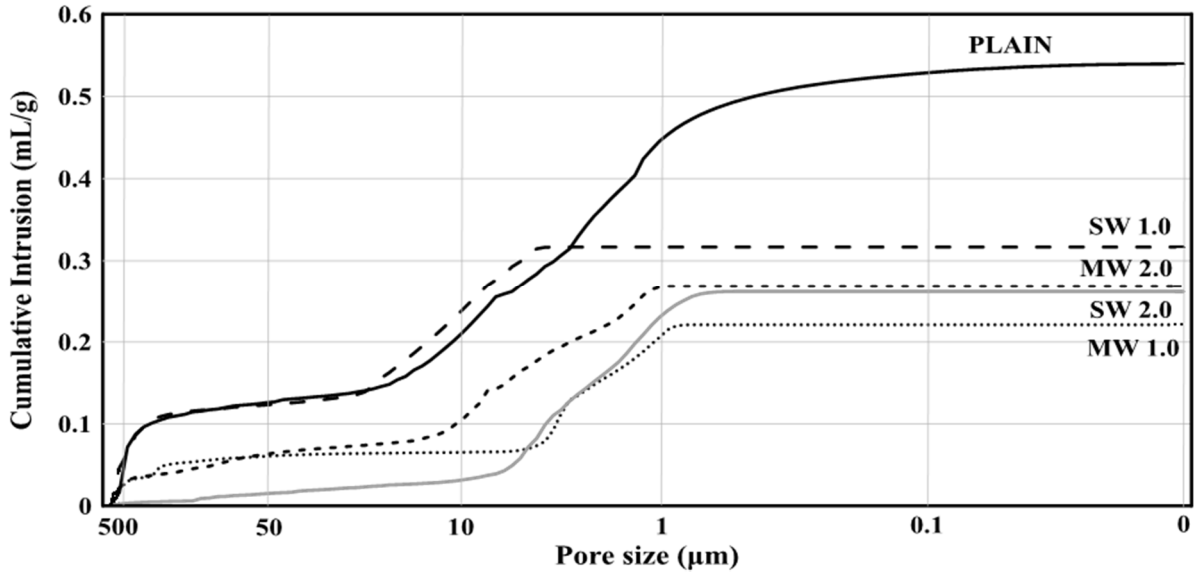

(**b**) After damage

Figure 13. Cumulative pore volume of CNT cementitious composites before and after immersion in 5% sulfuric solution: (**a**) before damage and (**b**) after damage.

4. Conclusions

This study aimed to evaluate the characteristics of deterioration caused by a sulfate in the CNT cementitious composites, and the following conclusions were drawn as follows;

1. When CNT was added to cement mortar, the compressive and flexural strengths further decreased compared to those of the specimen without CNT due to an increase in the amount of pores inside. In particular, it was found that relatively large pores with sizes ranging from 370 to 80 μm occurred due to the van der Waals force, and these pores resulted in the degradation of mechanical properties.
2. The electrical resistance of the CNT cementitious composites was significantly reduced by to up to 90%. In addition, the decrease in resistance value was greater in SWCNT cementitious composites than in MWCNT mixtures, indicating that SW exhibited more excellent electrical properties. The specimen subjected to deterioration resulting from sulfate ions showed a slight increase in the resistance compared to that before

the damage. This signifies that there will be no major complications in exhibiting self-sensing performance.

3. The incorporation of CNTs led to large pores forming in the cement mortar. However, as CNT particles with excellent chemical resistance prevented contact between cement hydrates and sulfate ions, the relaxation and breakage of hydrates affected the weight reduction rate and compressive strength decrease ratio, thereby improving the resistance to sulfate attack. In future studies, it is necessary to analyze the effect of the contact area between sulfuric acid and the cement structure on the pore size and pore distribution created by the incorporation of CNTs.

Author Contributions: Conceptualization, G.-C.L., S.-Y.S., and H.-D.Y.; methodology, G.-C.L. and S.-Y.S.; validation, G.-C.L., S.-Y.S., H.-D.Y., Y.K. and S.H.; formal analysis, G.-C.L., H.-D.Y., and S.H.; investigation, G.-C.L., S.-Y.S., and S.H.; resources, G.-C.L. and Y.K.; data curation, G.-C.L. and Y.K.; writing—original draft preparation, G.-C.L., Y.K., S.-Y.S., and S.H.; writing—review and editing, G.-C.L., S.-Y.S., H.-D.Y., and S.H.; visualization, S.H.; supervision, G.-C.L., S.-Y.S., and S.H.; project administration, G.-C.L. and S.-Y.S.; funding acquisition, G.-C.L., S.-Y.S., H.-D.Y., and S.H. All authors have read and agreed to the published version of the manuscript.

Funding: This research was supported by Basic Science Research Program through the National Research Foundation of Korea(NRF) funded by the Ministry of Education (No. 2018R1A4A1025953). The views expressed are those of authors and do not necessarily represent the sponsors.

Institutional Review Board Statement: Not applicable.

Informed Consent Statement: Not applicable.

Acknowledgments: This research was supported by Basic Science Research Program through the National Research Foundation of Korea (NRF) funded by the Ministry of Education (No. 2018R1A4A1025953).

Conflicts of Interest: The authors declare no conflict of interest.

References

1. Balageas, D.; Fritzen, C.P.; Güemes, A. *Structural Health Monitoring*, 1st ed.; Wiley-ISTE: London, UK, 2010.
2. Mitra, M.; Gopalakrishnan, S. Guided wave based structural health monitoring: A review. *Smart Mater. Struct.* **2016**, *25*, 053001. [CrossRef]
3. Yan, R.; Chen, X.; Mukhopadhyay, S.C. *Structural Health Monitoring*, 1st ed.; Springer: Berlin, Germany, 2017.
4. Bao, Y.; Chen, Z.; Wei, S.; Xu, Y.; Tang, Z.; Li, H. The state of the art of data science and engineering in structural health monitoring. *Engineering* **2019**, *5*, 234–242. [CrossRef]
5. Wang, C.S.; Wu, F.; Chang, F.K. Structural health monitoring from fiber-reinforced composites to steel-reinforced concrete. *Smart Mater. Struct.* **2001**, *10*, 548–552.
6. Silva-Muñoz, R.A.; Lopez-Anido, R.A. Structural health monitoring of marine composite structural joints using embedded fiber Bragg grating strain sensors. *Compos. Struct.* **2009**, *89*, 224–234. [CrossRef]
7. Wen, S.; Chung, D.D.L. Uniaxial compression in carbon fiber-reinforced cement, sensed by electrical resistivity measurement in longitudinal and transverse directions. *Cem. Concr. Res.* **2001**, *31*, 297–301. [CrossRef]
8. Wen, S.; Chung, D.D.L. Strain-sensing characteristics of carbon fiber-reinforced cement. *ACI Mater. J.* **2005**, *102*, 244–248.
9. Han, B.; Yu, X.; Kwon, E. A self-sensing carbon nanotube/cement composite for traffic monitoring. *Nanotechnology* **2009**, *20*, 445501. [CrossRef] [PubMed]
10. Azhari, F.; Banthia, N. Cement-based sensors with carbon fibers and carbon nanotubes for piezo resistive sensing. *Cem. Concr. Compos.* **2012**, *34*, 866–873. [CrossRef]
11. Galao, O.; Baeza, F.J.; Zornoza, E.; Garcés, P. Strain and damage sensing properties on multifunctional cement composites with CNF admixture. *Cem. Concr. Compos.* **2014**, *46*, 90–98. [CrossRef]
12. Kim, H.K.; Park, I.S.; Lee, H.K. Improved piezo resistive sensitivity and stability of CNT/cement mortar composites with low water–binder ratio. *Compos. Struct.* **2014**, *116*, 713–719. [CrossRef]
13. Lee, S.J.; You, I.; Zi, G.; Yoo, D.Y. Experimental investigation of the piezo resistive properties of cement composites with hybrid carbon fibers and nanotubes. *Sensors* **2017**, *17*, 2516. [CrossRef] [PubMed]
14. Yoo, D.Y.; You, I.; Lee, S.J. Electrical properties of cement-based composites with carbon nanotube, graphene, and graphite nanofiber. *Sensors* **2017**, *17*, 1064. [CrossRef]
15. Zhou, C.; Li, F.; Hu, J.; Ren, M.; Wei, J.; Yu, Q. Enhanced mechanical properties of cement paste by hybrid graphene oxide/carbon nanotubes. *Constr. Build. Mater.* **2017**, *1314*, 336–345. [CrossRef]

16. Yoo, D.Y.; You, I.; Youn, H.; Lee, S.J. Electrical and piezo resistive properties of cement composites with carbon nanomaterials. *J. Compos. Mater.* **2018**, *52*, 3325–3340. [CrossRef]
17. Dong, W.; Li, W.; Shen, L.; Sheng, D. Piezo resistive behaviours of carbon black cement-based sensors with layer-distributed conductive rubber fibres. *Mater. Des.* **2019**, *182*, 108012. [CrossRef]
18. Kim, G.M.; Nam, I.W.; Yang, B.; Yoon, H.N.; Lee, H.K.; Park, S. Carbon nanotube (CNT) incorporated cementitious composites for functional construction materials: The state of the art. *Compos. Struct.* **2019**, *227*, 111244. [CrossRef]
19. Nayak, S.; Das, S. A microstructure-guided numerical approach to evaluate strain sensing and damage detection ability of random heterogeneous self-sensing structural materials. *Comput. Mater. Sci.* **2019**, *156*, 195–205. [CrossRef]
20. Rovnaník, P.; Kusak, I.; Bayer, P.; Schmid, P.; Fiala, L. Comparison of electrical and self-sensing properties of Portland cement and alkali-activated slag mortars. *Cem. Concr. Res.* **2019**, *118*, 84–91. [CrossRef]
21. Choi, E.k.; Yuan, T.; Lee, J.Y.; Yoon, Y.S. Self-sensing Properties of Concrete with Electric Arc Furnace Slag and Steel Fiber. *J. Korean Soc. Hazard Mitig.* **2019**, *19*, 265–274. [CrossRef]
22. Lee, S.A.; Ann, K.Y. Evaluation on Sulfate Resistance of the High-durablility Culvert using CAC and GGBS. *J. Korea Concr. Inst.* **2018**, *30*, 465–472. [CrossRef]
23. Lee, G.C.; Choi, J.G.; Koh, K.T. The Effects of Mixture Rate and Aspect Ratio of Steel Fiber on Mechanical Properties of Ultra High Performance Concrete. *J. Korea Recycl. Constr. Resour. Inst.* **2017**, *5*, 14–20. [CrossRef]
24. Yoon, H.N.; Jang, D.I.; Lee, H.K.; Nam, I.W. Influence of carbon fiber additions on the electromagnetic wave shielding characteristics of CNT-cement composites. *Constr. Build. Mater.* **2020**, *269*, 121238. [CrossRef]
25. Choi, I.J.; Kim, J.H.; Chung, C.W. Mechanical Properties of Cement Paste with Nanomaterials. *J. Korea Inst. Build. Constr.* **2020**, *20*, 193–194.
26. Mehta, P.K. Mechanism of sulfate attack on portland cement concrete—Another look. *Cem. Concr. Res.* **1983**, *13*, 401–406. [CrossRef]
27. Wee, T.H.; Suryavanshi, A.K.; Wong, S.F.; Anisur Rahman, A.K.M. Sulfate resistance of concrete containing mineral admixtures. *Aci Mater. J.* **2000**, *97*, 536–549.
28. Shazali, M.A.; Baluch, M.H.; Al-Gadhib, A.H. Predicting residual strength in unsaturated concrete exposed to sulfate attack. *J. Mater. Civ. Eng.* **2006**, *18*, 343–354. [CrossRef]
29. Cavdar, A.; Yetgin, S. Investigation of mechanical and mineralogical properties of mortars subjected to sulfate. *Constr. Build. Mater.* **2010**, *24*, 2231–2242. [CrossRef]
30. Shanahan, N.; Zayed, A. Cement composition and sulfate attack: Part I. *Cem. Concr. Res.* **2007**, *37*, 618–623. [CrossRef]
31. Irassar, E.F.; Bonavetti, V.L.; González, M. Microstructural study of sulfate attack on ordinary and limestone portland cements at ambient temperature. *Cem. Concr. Res.* **2003**, *33*, 31–41. [CrossRef]
32. Yu, C.; Scrivener, K. Mechanism of expansion of mortars immersed in sodium sulphate solution. *Cem. Concr. Res.* **2013**, *43*, 105–111. [CrossRef]
33. Feng, P.; Garboczi, E.; Miao, C.; Bullard, J.W. Microstructural origins of cement paste degradation by external sulfate attack. *Constr. Build. Mater.* **2015**, *96*, 391–403. [CrossRef] [PubMed]
34. Sarkar, S.L.; Mahadevan, S.; Meeussen, J.C.L.; van der Sloot, H.; Kosson, S. Numerical simulation of cementitious materials degradation under external sulfate attack. *Cem. Concr. Compos.* **2010**, *32*, 241–252. [CrossRef]
35. Al-Akhras, N.M. Durability of metakaolin concrete to sulfate attack. *Cem. Concr. Res.* **2006**, *36*, 1727–1734. [CrossRef]
36. Haufe, J.; Vollpracht, A. Tensile strength of concrete exposed to sulfate attack. *Cem. Concr. Res.* **2019**, *116*, 81–88. [CrossRef]
37. Yun, H.D.; Youn, D.A.; Kim, J.H.; Lee, G.C.; Seo, S.Y. Tensile and Strain-sensing Properties of Hybrid Fibers Reinforced Strain-hardening Cement Composite (Hy-SHCC) with Different Carbon Nanotube (CNT) Dosages. *J. Korea Concr. Inst.* **2020**, *32*, 285–293. [CrossRef]
38. Lee, G.C.; Kim, Y.M.; Hong, S.W. Influence of Powder and Liquid Multi-Wall Carbon Nanotubes on Hydration and Dispersion of the Cementitious Composites. *Appl. Sci.* **2020**, *10*, 7948. [CrossRef]
39. Makar, J.M.; Margeson, J.C.; Luh, J. Carbon nanotube/cement composites—Early results and potential applications. In Proceedings of the 3rd International Conference on Construction Materials: Performance, Innovations and Structural Implications, Vancouver, BC, Canada, 22–24 August 2005.
40. Li, G.Y.; Wang, P.M.; Zhao, X. Mechanical behavior and microstructure of cement composites incorporating surface-treated multi-walled carbon nanotubes. *Carbon* **2005**, *43*, 1239–1245. [CrossRef]
41. Vaisman, L.; Wagner, H.D.; Marom, G. The role of surfactants in dispersion of carbon nanotubes. *Adv. Colloid Interface Sci.* **2006**, *128*, 37–46. [CrossRef]
42. Yu, J.; Grossiord, N.; Koning, C.E.; Loos, J. Controlling the dispersion of multi-wall carbon nanotubes in aqueous surfactant solution. *Carbon* **2007**, *45*, 618–623. [CrossRef]
43. Cwirzen, A.; Habermehl-Cwirzen, K.; Penttala, V. Surface decoration of carbon nanotubes and mechanical properties of cement/carbon nanotube composites. *Adv. Cem. Res.* **2008**, *20*, 65–73. [CrossRef]
44. Sanchez, F.; Ince, C. Microstructure and macroscopic properties of hybrid carbon nanofiber/silica fume cement composites. *Compos. Sci. Technol.* **2009**, *69*, 1310–1318. [CrossRef]
45. Luo, Y.; Heng, Y.; Dai, X.; Chen, W.; Li, J. Preparation and photocatalytic ability of highly defective carbon nanotubes. *J. Solid State Chem.* **2009**, *182*, 2521–2525. [CrossRef]

46. Ma, P.-C.; Siddiqui, N.A.; Marom, G.; Kim, J.-K. Dispersion and functionalization of carbon nanotubes for polymer-based nanocomposites: A review. *Compos. Part A Appl. Sci. Manuf.* **2010**, *41*, 1345–1367. [CrossRef]
47. Konsta-Gdoutos, M.S.; Metaxa, Z.S.; Shah, S.P. Multi-scale mechanical and fracture characteristics and early-age strain capacity of high performance carbon nanotube/cement nanocomposites. *Cem. Concr. Compos.* **2010**, *32*, 110–115. [CrossRef]
48. Kim, B.R.; Lee, H.K.; Kim, E.; Lee, S.H. Intrinsic electromagnetic radiation shielding/absorbing characteristics of polyaniline-coated transparent thin films. *Synth. Met.* **2010**, *160*, 1838–1842. [CrossRef]
49. Nochaiya, T.; Chaipanich, A. Behavior of multi-walled carbon nanotubes on the porosity and microstructure of cement-based materials. *Appl. Surf. Sci.* **2011**, *257*, 1941–1945. [CrossRef]
50. Collins, F.; Lambert, J.; Duan, W.H. The influences of admixtures on the dispersion, workability, and strength of carbon nanotube–OPC paste mixtures. *Cem. Concr. Compos.* **2012**, *34*, 201–207. [CrossRef]
51. Ha, S.J.; Kang, S.T.; Lee, J.H. Strength of CNT Cement Composites with Different Types of Surfactants and Doses. *J. Korea Inst. Struct. Maint. Insp.* **2015**, *19*, 99–107. [CrossRef]
52. KS L 5201. *Portland Cemen*; Korean Agency for Technology and Standards: Maengdong-myeon, Korea, 2016; pp. 3–15.
53. KS L ISO 679. *Methods of Testing Cements—Determination of Strength*; Korean Agency for Technology and Standards: Maengdong-myeon, Korea, 2016; pp. 12–16.
54. KS F 2560. *Chemical Admixtures for Concrete*; Korean Agency for Technology and Standards: Maengdong-myeon, Korea, 2007; pp. 1–3.
55. Bellmann, F.; Möser, B.; Stark, J. Influence of sulfate solution concentration on the formation of gypsum in sulfate resistance test specimen. *Cem. Concr. Res.* **2006**, *36*, 358–363. [CrossRef]
56. Bae, S.H.; Park, J.I.; Lee, K.M. Influence of Mineral Admixtures on the Resistance to Sulfuric Acid and Sulfate Attack in Concrete. *J. Korea Concr. Inst.* **2010**, *22*, 219–228. [CrossRef]
57. Elyamany, H.E.; Elmoaty, A.M.A.; Elshaboury, A. M Magnesium sulfate resistance of geopolymer mortar. *Constr. Build. Mater.* **2018**, *184*, 111–127. [CrossRef]
58. JSTMC 7401. *Method of Test for Chemical Resistance of Concrete in Aggressive Solution*; Japanese Industrial Standard: Tokyo, Japan, 1999.
59. Kwon, S.J.; Na, U.J. An experimental Study on Characteristics of Averaged Electromagnetic Properties considering Moisture Changes in Cement Mortar. *J. Korea Concr. Inst.* **2009**, *21*, 199–207. [CrossRef]